Journal of Coordination Chemistry

ISSN: 0095-8972 (Print) 1029-0389 (Online) Journal homepage: http://www.tandfonline.com/loi/gcoo20

Acetate platinum(II) compound with 5,7-ditertbutyl-1,2,4-triazolo[1,5-a]pyrimidine that overcomes cisplatin resistance: structural characterization, in vitro cytotoxicity, and kinetic studies

Kamil Hoffmann, Iwona Łakomska, Joanna Wiśniewska, Anna Kaczmarek-Kędziera & Joanna Wietrzyk

To cite this article: Kamil Hoffmann, Iwona Łakomska, Joanna Wiśniewska, Anna Kaczmarek-Kędziera & Joanna Wietrzyk (2015) Acetate platinum(II) compound with 5,7-ditertbutyl-1,2,4-triazolo[1,5-a]pyrimidine that overcomes cisplatin resistance: structural characterization, in vitro cytotoxicity, and kinetic studies, Journal of Coordination Chemistry, 68:17-18, 3193-3208, DOI: 10.1080/00958972.2015.1070954

To link to this article: http://dx.doi.org/10.1080/00958972.2015.1070954

Journal of Coordination Chemistry, 2015
Vol. 68, Nos. 17–18, 3193–3208, http://dx.doi.org/10.1080/00958972.2015.1070954

Acetate platinum(II) compound with 5,7-ditertbutyl-1,2,4-triazolo[1,5-*a*]pyrimidine that overcomes cisplatin resistance: structural characterization, *in vitro* cytotoxicity, and kinetic studies

KAMIL HOFFMANN†, IWONA ŁAKOMSKA*†, JOANNA WIŚNIEWSKA‡, ANNA KACZMAREK-KĘDZIERA‡ and JOANNA WIETRZYK§

†Bioinorganic Chemistry Research Group, Faculty of Chemistry, Nicolaus Copernicus University in Toruń, Toruń, Poland
‡Faculty of Chemistry, Nicolaus Copernicus University in Toruń, Toruń, Poland
§Ludwik Hirszfeld Institute of Immunology and Experimental Therapy, Polish Academy of Sciences, Wrocław, Poland

(*Received 1 April 2015; accepted 22 June 2015*)

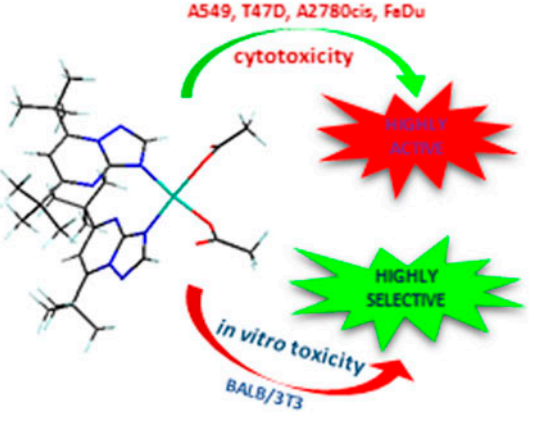

The reaction of silver acetate with *cis*-[$PtI_2(dbtp)_2$], where dbtp = 5,7-ditertbutyl-1,2,4-triazolo-[1,5-*a*]pyrimidine, yielded *cis*-[$Pt(OOCCH_3)_2(dbtp)_2$]·dmf (**1**). The complex has been analyzed by multinuclear magnetic resonance (^1H, ^{13}C, ^{15}N), IR, and Raman. The compound formed two rotamers in $CDCl_3$ and its spatial structures have been optimized using computational calculation. It was found that head-to-tail rotamer (**1a**) is more stable than its head-to-head counterpart (**1b**). *In vitro* antiproliferative activity against four tumor cell lines (A549, T47D, FaDu, and A2780cis) revealed in all cases significant cytotoxicity (IC_{50} = 0.26–1.80 μM), possessing IC_{50} values at least fivefold lower than cisplatin, carboplatin, and oxaliplatin (except A2780cis). The remarkable *in vitro* activity against T47D and A2780cis suggested the ability to overcome cisplatin resistance in these types of tumor cells. In addition, *in vitro* toxicity was evaluated against BALB/3T3 and has shown

*Corresponding author. Email: iwolak@chem.umk.pl

Dedicated to Professor Rudi van Eldik with the very best wishes of the authors for all his future endeavors.

that the lipophilic platinum(II) complex (**1**) inhibits cell proliferation weaker than cisplatin and oxaliplatin. Additionally, *cis*-[Pt(OOCCH$_3$)$_2$(dbtp)$_2$]·dmf exhibited selective activity, in contrast to cisplatin or oxaliplatin.

Keywords: Platinum(II) complexes; Acetate; ^{15}N NMR; Hydrolysis; *In vitro* cytotoxicity; Computational calculation

1. Introduction

The chemistry of 1,2,4-triazolo[1,5-*a*]pyrimidine ligands is of interest because they have several nitrogens with accessible lone pairs to bind with metal ions [1–7]. Furthermore, the diversity can be increased by substituting the pyrimidine ring functional groups. The presence of a number of coordination sites is interesting from the point of view of coordination chemistry, making it possible to obtain interesting and diverse structures and properties of coordination compounds.

An example of disubstituted 1,2,4-triazolo[1,5-*a*]pyrimidines is 5,7-ditertbutyl-1,2,4-triazolo[1,5-*a*]pyrimidine (dbtp) (figure 1); some non-platinum coordination compounds such as Ru(III), Pd(II), or Zn(II) are known and have been reviewed [8–10]. The ligand inhibited the proliferation of 64–76% of human lung adenocarcinoma cells (A549) as well as cisplatin-resistant human breast epithelial tumor cells (T47D), at the highest tested concentration 100.00 μg mL^{-1} [11]. More recently, dbtp has been shown to exhibit synergistic activity with platinum ion in the case of *cis*-[PtI$_2$(dbtp)$_2$] [12], *cis*-[PtCl$_2$(dbtp)$_2$] [13], and [PtCl$_4$(dbtp)$_2$] [14]. The two latter compounds were twofold more *in vitro* active than commonly used *cisplatin* against human rectal or bladder cancer cells. Careful comparison of *in vitro* cytotoxic data for a series of chlorido platinum(II/IV) compounds containing disubstituted triazolopyrimidine has shown the strong impact of alkyl groups in the 5,7 positions [15]. The best antitumor parameters were demonstrated by complexes with dbtp, which suggests that the presence of bulky *tert*-butyl substituents in the heterocyclic ring might be a major factor in the cytotoxicity of platinum compounds.

Unfortunately, these halogeno species exhibited rather low solubility in fluids; therefore, we decided to replace the chloride anions in *cis*-[PtCl$_2$(dbtp)$_2$] by more stable malonate [11] or malate [14]. As reported, the spectroscopic data for both complexes and X-ray of the malonate-analog confirmed monodentate coordination of dbtp via N(3) and monodentate

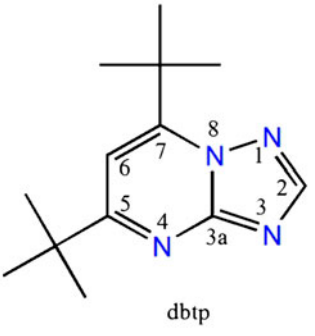

dbtp

Figure 1. The formula of dbtp and its IUPAC ring-numbering system.

mode of each carboxylate. In the case of *in vitro* cytotoxicity against A549 (human lung adenocarcinoma) and T47D (cisplatin-resistant human breast tumor cells), the compounds had two or fourfold lower IC_{50} values than cisplatin, suggesting that they are able to overcome cisplatin-resistance mechanisms in that breast tumor cell line. Furthermore, [Pt(malonate)(dbtp)$_2$] [11] also showed remarkable *in vitro* activity toward human bladder, and colorectal cancer or acute promyelocytic leukemia cells.

To develop more soluble and lower toxic platinum(II) coordination compounds, we decided to exploit monodentate acetate. Consequently, in this manuscript, the attention was focused on: i) synthesis and spectroscopic characterization (IR, Raman, ^{1}H, ^{13}C, ^{15}N NMR) of *cis*-[Pt(OOCCH$_3$)$_2$(dbtp)$_2$]·dmf, ii) isomeric structure determination based on computational methods, iii) determination of partition coefficient and *in vitro* antiproliferative activity, and iv) kinetic studies of hydrolysis.

2. Experimental

2.1. *Materials*

3-Amino-1,2,4-triazole (98%), 2,2,6,6-tetramethyl-3,5-heptanedione (98%), and K_2PtCl_4 (98%) were purchased from Aldrich, whereas inorganic salts and solvents of analytical grade were purchased from POCh Gliwice (Poland). 5,7-Ditertbutyl-1,2,4-triazolo[1,5-*a*]-pyrimidine (dbtp) was prepared according to the Bülow and Haas method [16]. Silver(I) acetate (98%) was purchased from Merck.

2.2. *Instrumentation*

The C, H, and N contents were determined by elemental semi-microanalysis. IR spectra were measured with a Perkin–Elmer Spectrum 2000 FTIR spectrometer using KBr (400–4000 cm^{-1}) and polyethylene disks (100–400 cm^{-1}). Raman spectra were collected at room temperature using a Horiba LabRAM HR confocal microscope system with a 532-nm green laser. The UV–vis measurements for determination of lipophilicity were obtained on an UVD-2950 UV–vis spectrophotometer using 1.0-cm pathlength quartz cuvettes (1.5 mL).

NMR spectra were recorded at 298 K in $CDCl_3$ solutions (**1**) or D_2O (kinetic hydrolysis products) on a Bruker Avance III 700 or 400 MHz NMR. The reference standard was TMS for ^{1}H and ^{13}C, CH_3NO_2 (external) for ^{15}N. The ^{1}H{^{13}C} and ^{1}H{^{195}Pt} NMR spectra were obtained using the absolute value gradient heteronuclear multiple quantum correlation and/or the gradient heteronuclear multiple bond correlation (HMBC) methods; ^{1}H{^{15}N} correlation spectra were performed using the gradient-enhanced IMPACT–HMBC method.

ESI-MS measurements of the kinetic hydrolysis products were performed on a Synapt G2-S mass spectrometer using the following parameters: spray voltage 1.8 kV, capillary temperature 150 °C, ion transfer capillary voltage 20 V, and tube lens offset 0 V. ESI-MS spectra for reaction aqueous solutions were recorded for the mass range *m/z* 100–1000.

2.3. *Preparation of platinum(II) complex (1)*

Substrate for further synthesis of *cis*-[PtI$_2$(dbtp)$_2$] was prepared by the published method [12]. A suspension of *cis*-[PtI$_2$(dbtp)$_2$] (0.150 g, 0.16 mmol) in 60 mL mixture of dmf and

methanol in ratio 1 : 5 (v/v) was treated with silver(I) acetate (0.054 g, 0.32 mmol). The reaction mixture was stirred in the dark at 40 °C for 24 h. The resulting silver(I) iodide was removed by centrifugation and filtration. The clear filtrate was evaporated to dryness and freeze-dried. Yield: 0.108 g; (86%). The existence of one dmf molecule out of the Pt(II) coordination sphere was confirmed by semi-microanalysis and appearance of characteristic resonance lines in the ^{13}C NMR spectra. Anal. Calc. for $C_{33}H_{53}N_9O_5Pt$ (%): H, 6.28; N, 14.81. Found: H, 6.30; N, 14.41. Full spectroscopic data for (**1a**) and (**1b**) have been collected in Supplemental online material (SI_1).

2.4. *Computational details*

All the theoretical calculations have been performed within the Gaussian09 package of programs [17]. For geometry optimization, the B3LYP-D3 functional has been applied with the cc-pVDZ basis set for light elements and cc-pVDZ-PP for platinum [18]. The initial geometry was designed on the basis of known crystal structures of *cis*–$[PtI_2(dbtp)_2]$ [12] and $[Pt(mal)(dbtp)_2]$ [11] and the full conformational analysis has been performed for rotation of the acetate groups. Only the lowest energy structures are presented in the current contribution. The character of the stationary points was confirmed by the harmonic frequency analysis.

2.5. In vitro *cytotoxicity*

2.5.1. Cell culture. Antiproliferative activity of tested compounds was studied *in vitro* for human lung adenocarcinoma epithelial cell line (A549), cisplatin-resistant human ductal breast epithelial tumor cell (T47D), human pharyngeal squamous carcinoma (FaDu), cisplatin-resistant human ovarian tumor cell (A2780cis), and normal murine embryonic fibroblast cells (BALB/3T3). Cells were cultured in RPMI–1640 + OPTI–MEM (1 : 1) medium (A549, T47D) (IIET, Poland), Dulbecco medium (BALB/3T3) (Gibco), RPMI–1640 + GlutaMAX medium (FaDu) (IIET, Poland), and RRMI–1640 medium (A2780cis) (IIET, Poland). RPMI–1640 + OPTI–MEM medium was supplemented with 5% FBS (HyClone), L–glutamine 2 mM, and 8 μg mL^{-1} insulin (T47D) (Sigma-Aldrich, Poland); Dulbecco medium was supplemented with 10% FBS (HyClone) and 2 mM L–glutamine (Sigma-Aldrich, Poland) (BALB/3T3); RPMI–1640 + GlutaMAX medium was supplemented with 10% FBS (HyClone), 1 mM sodium puryvate, and 1% amino acids (Sigma-Aldrich, Poland); RPMI–1640 medium for A2780cis was supplemented with 10% FBS (HyClone) and 2 mM L–glutamine. Mentioned culture media contained antibiotics: 100 U mL^{-1} penicillin and 100 μg mL^{-1} streptomycin (Polfa–Tarchomin, Poland). All cell lines were grown at 37 °C in a humidified atmosphere with 5% CO_2.

2.5.2. Cell growth inhibition assay. Cells were plated in 96-well sterile plates (Sarstedt, Costar) at a density of 10^4 cells per well (in 100 μL of culture medium) and incubated for 24 h. The tested compound was added in final concentrations ranging from 0.1 to 100 μg mL^{-1}, and the incubation was continued for an additional 72 h. The results of cytotoxic activity *in vitro* were expressed as an IC_{50} [the dose of compound (in μM) that inhibits proliferation rate of tumor cells by 50%] compared to the untreated control cells. IC_{50} values are the average of 3–5 independent determinations. The details of this technique

were described by Skehan [19]. The tests of the antiproliferative activity *in vitro* against both cell lines were performed with the SRB (sulforhodamine B) test using an automated microplate reader (Synergy H4 photometer, BioTek Instruments, USA) [13].

2.6. *Determination of lipophilicity*

The lipophilicity (log *P*) of the compound was determined using the shake-flask method [20]. Aqueous (0.9% w/v) sodium chloride and organic (*n*-octanol) phases were saturated for 1 week. Drugs were dissolved at a concentration of 0.30 mg mL^{-1} in 2.5 mL of saturated *n*-octanol, except cisplatin was dissolved in the aqueous phase. An equal volume of immiscible solvent was added and the solutions were mixed mechanically in plastic tubes for 0.5 h. Samples were centrifuged (6000 rpm, 15 min). After separation, the phases were analyzed by UV–vis spectroscopy to determine the amount of compound in each phase. The absorption values before and after shaking were compared based on the Lambert–Beer Law; the partition coefficient in both phases for each compound was calculated to determine the log *P* values. The procedures were repeated five times.

2.7. *Kinetics of hydrolysis*

2.7.1. Measurement details. Kinetic measurements were performed in a quartz Tandem cuvette, which contained 1.0 mL of an aqueous 1.3×10^{-4} M platinum(II) solution and 1.0 mL of a solution of sodium hydroxide (OH^-, ClO_4^-, Na^+) at an appropriate concentration. The reaction rate was followed as an increase in absorbance in the charge-transfer transition band *versus* time and was analyzed at a variety of OH^- concentrations: $[Pt^{II}] = 6.5 \times 10^{-5}$ M; $[OH^-] = 0.02$–0.09 M; $I = 0.1$ M (OH^-, ClO_4^-, Na^+); $T = 298$, 303, 308, and 313 K; and $\lambda = 340$ nm. In a separate series of experiments, kinetic measurements were performed in a HEPES buffer solution (H^+, ClO_4^-, Na^+) in acidic media. As in the case of hydrolysis, sodium perchlorate salt was used to maintain an appropriate ionic strength $I = 0.1$ M (H^+, ClO_4^-, Na^+, $A^-_{(HEPES)}$)). The other experimental conditions were as follows: $[Pt^{II}] = 6.5 \times 10^{-5}$ M; pH 5–7; $I = 0.1$ M (H^+, ClO_4^-, Na^+, $A^-_{(HEPES)}$); $T = 308$ K; and $\lambda = 340$ nm. Kinetic data were acquired and processed using UVPC personal spectroscopy software. The kinetic traces in hydrolysis as well as the reaction in acidic media run according a two-exponential equation. The pseudo-first-order rate constants for two consecutive reaction schemes were calculated using a non-linear fitting procedure for multi-exponential absorbance dependence *versus* time. At least three kinetic runs were recorded for every combination of reagent concentrations, and the rate constants are reported as average values. Analyses of kinetic products were performed using ^1H, ^{13}C NMR, and ESI-MS.

3. Results and discussion

3.1. *NMR spectroscopy*

The ^1H NMR spectra of the ligand and the acetate platinum(II) complex in $CDCl_3$ were recorded and compared. The highest changes of the chemical shift in the ^1H NMR spectra were observed for H(2) and H(6). Two characteristic signals were detected at 8.99 and

Table 1. ^{1}H, ^{13}C NMR chemical shifts (δ) of platinum(II) complex (coordination shifts in parentheses).

	^{1}H		^{13}C				
Compound	H(2)	H(6)	C(2)	C(3a)	C(5)	C(6)	C(7)
(**1a**)	8.99 (+0.55)	6.88 (−0.14)	153.8 (−0.5)	153.4 (−2.6)	177.2 (+1.6)	104.8 (+1.6)	158.9 (+1.5)
(**1b**)	8.67 (+0.23)	7.13 (+0.11)	153.2 (−1.1)	152.9 (−3.1)	178.2 (+2.6)	106.4 (+3.2)	159.9 (+2.5)

6.88 ppm. However, the spectrum changed over time, and after 1 h, two sets of resonances (**1a**, **1b**) were observed (table 1). The ^{1}H NMR chemical shifts of H(2) and H(6) were at 8.67 and 7.13 ppm for (**1b**). Integration of ^{1}H NMR signals (295 K) demonstrated that in $CDCl_3$, 82% of (**1a**) and 18% of (**1b**) exist in equilibrium. The two complexes were probably rotamers: head-to-tail and head-to-head formed by the restrained rotation of the heterocycle ligand (dbtp) around the Pt-N(3) or Pt-N(3′) bond, caused by steric hindrance of the bulky *tert*-butyl groups in the N-ligands. The effect of rotational isomers was observed also in NMR spectra of two complexes: $[PtCl_4(dbtp)_2]$ [14] and *cis*-$[PdCl_2(dbtp)_2]$ [21].

The biggest coordination shift calculated for H(2) from the triazole ring (maximum 0.55 ppm) suggests N(1) or N(3) engaged in formation of the Pt–N bond. However, a clear answer regarding coordination sites was obtained from ^{1}H–^{15}N NMR spectrum. As a result of coordinating triazolopyrimidine to Pt(II), the resonance of N(3) has shielding (99 and 103 ppm for (**1b**) or (**1a**), respectively) (figure 2). Similar coordination shift on N(3) was noticed for dicarboxylate Pt(II) complexes, $[Pt(malate)(dbtp)_2]$ (96 ppm) [12], and $[Pt(malonate)(dbtp)_2]$ (99.6 ppm) [11].

For ^{13}C NMR, a clear pattern of the coordination shift for (**1a**) and (**1b**) has been observed. C(2) and C(3a) signals are shielded (0.5–3.1 ppm), whereas C(5), C(6), and C(7) signals are deshielded (1.5–3.2 ppm). Two more singlets at 23.1 ppm and 179.60 ppm were observed from carbons (from methyl and carboxyl groups, respectively) of monodentate acetate.

3.2. *Infrared and Raman spectroscopy*

In the IR spectra of Pt(II) acetate complex, one band assignable to υ_{as}(C=O) was found at 1638 cm^{-1}, whereas the maximum of the υ_s(C–O) vibration was detected at 1438 cm^{-1}. The mode of carboxylate coordination to a metal was determined based on $\Delta_{coord.}(\upsilon_{as}(C{=}O)–\upsilon_s(C–O))$. In our case, calculated Δ_{coord} was greater (200 cm^{-1}) than the corresponding parameter for sodium acetate (164 cm^{-1}), suggesting monodentate coordination of acetate [22]. Additionally, the two bands expected for υ(Pt–O) in *cis* conformation at 529 and 519 cm^{-1} were observed.

The second type of ligands coordinated to the Pt(II) in the complex showed two characteristic bands. The most intense υ_{pyrim} stretch and υ_{triaz} overall ring vibration occurred at 1617 and 1543 cm^{-1}, respectively. The maxima of these bands were shifted into the spectra

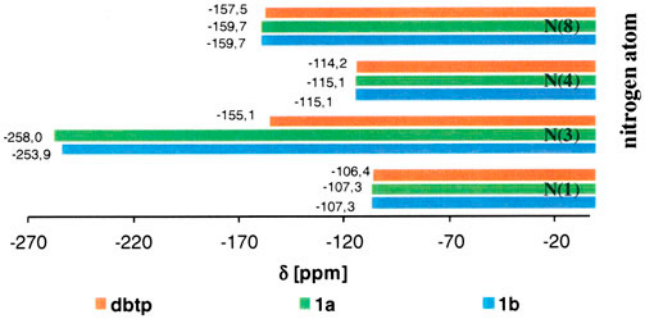

Figure 2. ^{15}N NMR data for dbtp and both rotamers.

of complex to higher frequencies after complexation. Moreover, the $\upsilon_{(Pt-N)}$ vibration that indirectly confirmed coordination of N-donor ligands to the metal center was observed at 226 cm^{-1}.

Some bands detected in the infrared spectrum of the Pt(II) acetate complex also appeared in the appropriate Raman spectrum. The $\upsilon_{(Pt-N)}$ band was observed at 231 cm^{-1} and the υ(Pt–O) bands at 517 cm^{-1}. The maxima of the N-donor ligands were found at 1608–1538 cm^{-1}. Unfortunately, these bands were partially overlapped by the very strong υ_{as}(C=O) band at 1675 cm^{-1}. The υ_s(C–O) vibration observed in the IR spectrum was not detected in Raman spectrum because of overlapping by band at about 1367 cm^{-1}, which most likely belongs to the skeletal vibrations of a purine ring [23].

3.3. *Optimized structures by computational calculation*

As no single crystal for X-ray diffraction studies could be obtained, the structures of the two rotamers, head-to-tail (**1a**) and head-to-head (**1b**), have been optimized using DFT as shown in figure 3 Ref. [24]. A direct comparison with experimental data appeared possible for *cis*-[PtI_2(dbtp)$_2$] [12] and [Pt(malonate)(dbtp)$_2$] [11], whose structures had been previously reported. Thus, the structures of these compounds were used as starting structures to generate initial models for the remaining compounds. The comparison of some structural details for *cis*-[PtI_2(dbtp)$_2$] [12] and [Pt(malonate)(dbtp)$_2$] [11], calculated and observed, shows good agreement with a relative error below 3% (table 2).

The structures showed that the heterocycles of dbtp are planar. Selected bond lengths and angles for optimized structures of the two rotamers are presented in table 3. For both rotamers, a slightly disordered square planar coordination sphere of Pt(II) is formed by two monodentate dbtp and acetate in *cis* configuration. Different arrangements of the triazolopyrimidines in the coordination sphere are observed. In rotamer (**1a**), dbtp is in a head-to-tail orientation, whereas in (**1b**), N-donor ligands were found in a head-to-head

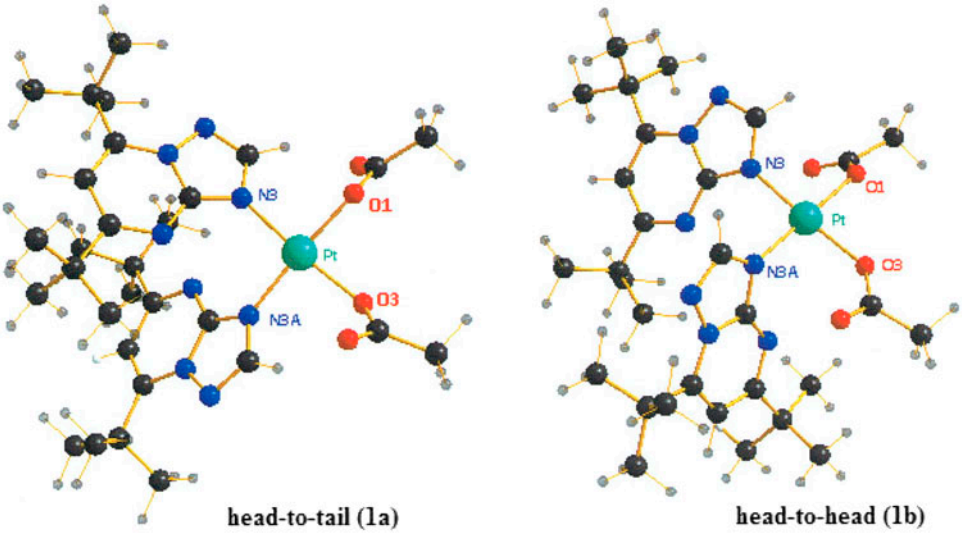

Figure 3. Energy-optimized structures of head-to-tail (**1a**) and head-to-head (**1b**).

Table 2. Comparison of crystallographic data for *cis*-[$PtI_2(dbtp)_2$] and [Pt(malonate)$(dbtp)_2$] with the computational calculation.[a]

Experimental Bond lengths (Å)			Calculated Bond lengths (Å)		
	cis–[$PtI_2(dbtp)_2$] [12]	[Pt(malonate) $(dbtp)_2$] [11]		*cis*-[$PtI_2(dbtp)_2$] [12]	[Pt(malonate) $(dbtp)_2$] [11]
Pt–N3	2.055	1.999	Pt–N3	2.093 (1.8%)	2.035 (1.8%)
Pt–N3A	2.055	2.006	Pt–N13	2.093 (1.8%)	2.037 (1.6%)
Pt–O2/I1	2.579	2.004	Pt–O3/I1	2.648 (2.7%)	1.995 (0.2%)
Pt–O3/I1A	2.579	1.998	Pt–O2/I1A	2.648 (2.7%)	1.998 (0.3%)
	Angles (°)			*Angles (°)*	
N3A–Pt–N3	89.29	95.04	N3A–Pt–N3	91.27 (2.2%)	95.63 (0.6%)
N3A–Pt–O2/I1	89.90	85.56	N3A–Pt–O2/I1	88.69 (1.3%)	85.38 (0.2%)
N3–Pt–O3/I1A	89.90	87.40	N3–Pt–O3/I1A	88.69 (1.3%)	85.23 (2.5%)
O3/I1A–Pt–O2/I1	90.93	91.98	O3/I1A–Pt–O2/I1	91.56 (0.7%)	93.78 (2.0%)

[a]Percentage in the parentheses represents the relative error between experimental and calculated values.

Table 3. Selected bond lengths (Å) and angles (°) for the optimized structures of two rotamers of *cis*-[$Pt(OOCCH_3)_2(dbtp)_2$].

	Head-to-tail (**1a**)	Head-to-head (**1b**)
	Bond lengths (Å)	
Pt–N3	2.034	2.027
Pt–N3A	2.034	2.020
Pt–O1	2.018	2.021
Pt–O3	2.018	2.014
	Angles (°)	
N3–Pt–N3A	93.34	90.64
N3A–Pt–O3	90.85	95.51
N3–Pt–O1	90.85	89.53
O1–Pt–O3	85.45	84.40

position. The difference in the orientation of dbtp in (**1a**) and (**1b**) results in large changes in the N3–Pt–N3A and N3A–Pt–O3 angles, 93.34° (**1a**) or 90.64° (**1b**), and 90.85° (**1a**), and 95.51° (**1b**), respectively. Computed values of the minimized energy showed that the head-to-tail rotamer (**1a**) is slightly more stable than the head-to-head one (**1b**) ($\Delta E_{(E(1a)\text{-}E(1b)} = -7.32$ kcal/mol). These results are in agreement with our assumptions during the analysis of NMR spectra.

3.4. *Kinetics of hydrolysis and aquation of cis-[Pt(OOCCH$_3$)(dbtp)$_2$]·dmf*

Substitution reactions of the leaving groups from inner coordination sphere of platinum(II) are key reactions of platinum drugs in human cells. The cytotoxic activity of platinum(II) in cells results in their efficiency to undergo a series of hydrolysis reactions, forming species including mono and diaqua species, where one and two molecules of the leaving groups have been replaced in the substitution reactions by a water molecule. The reactions were investigated in a basic perchlorate media ($[OH^-] = 0.01$–0.1 M, $[ClO_4^-] = 0.1$ M, $I = 0.1$ M, $T = 298$, 303, 308, 313 K, $\lambda = 340$ nm). Reaction proceeded via two consecutive reactions, in which the first and second carboxylates are substituted (figure 4).

The kinetic traces followed two-exponential function according to the equation $A = A_o + A_1\exp(-k_{1obs}t) + A_2\exp(-k_{2obs}t)$, where A = absorbance, t = time, and $k_{1(2)obs}$ = observed rate

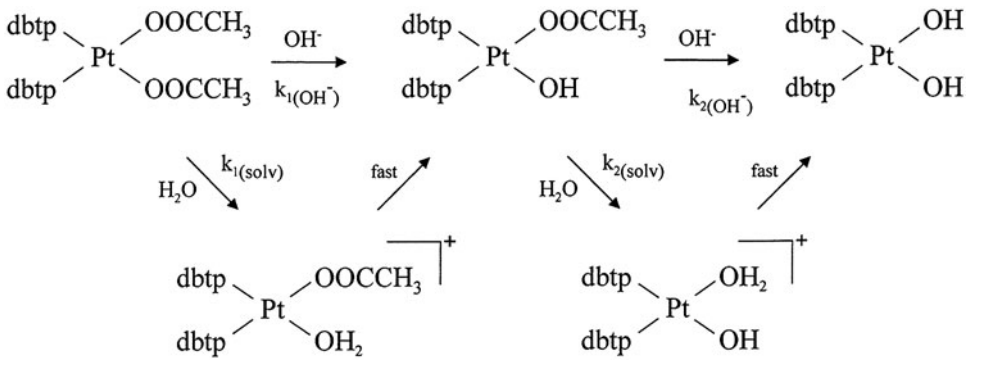

Figure 4. Possible pathways of the hydrolysis and aquation reactions of *cis*-$[Pt(OOCCH_3)_2(dbtp)_2]$·dmf.

constants for the first and second steps, respectively. The first step is not hydrolysis and kinetic data were not dependent of $[OH^-]$, but only fluctuated by changing of the OH^- concentration and temperature. This process did not proceed with any isosbestic points and only revealed an increase in absorbance of the overall spectra in ultra-violet region during the first 2–3 min after mixing. The estimated first-order rate constant is $1.8 \times 10^{-2}\ s^{-1}$ at 298 K (Supplementary data: SI_2). This initiated process resulted in a decrease in solubility of a free triazolopyrimidine ligand in perchlorate media that appeared as impurities in complex salt or as increase in absorbance with increasing temperature in the reaction solutions during the first few minutes after mixing.

The second process is the first step of base hydrolysis. Each reaction step of hydrolysis of platinum(II) complex with carboxylate as a leaving group proceeded according to two reaction paths, spontaneous and OH^- catalyzed hydrolysis (figure 4). The pseudo-first-order rate constants (k_i) can be expressed as

$$k_i = k_{i(OH^-)}[OH^-] + k_{i(solv)}$$

where i = 1 (first step), 2 (second step), k_i is the observed rate constant, $k_{i(OH^-)}$ is the second-order rate constant for OH^- catalyzed process, and $k_{i(solv)}$ is the first-order rate constant for the spontaneous process. The rate constants ($k_{i(OH^-)}$ and $k_{1(solv)}$) for the first step of the hydrolysis are presented in table 4.

Similar dependence is observed for aquation at pH 5–7 in HEPES buffer solution. In HEPES buffer solutions in acidic media ($pK_{a1} = 3$, ($k_{i(OH^-)}$·$pK_{a1} = 7.48$ [25]), the reaction proceeds with similar rate for the spontaneous process as in basic perchlorate media, indicating that both hydrolysis and aquation proceed according to the same mechanism and the same groups leave the inner coordination sphere of platinum(II) complex (table 5). The dominant reaction path is the substitution of each carboxylate by a solvent molecule in the spontaneous reaction ($k_{i(solv)}$), which is faster than the hydroxo ion catalyzed substitution $[OH^-]$).

The hydrolysis of the leaving group is necessary to provide a labile site (coordinated water) for substitution chemistry that leads to introduction of the N-donor DNA base into the inner coordination sphere in cancer cells. This process in the *cis*-$[Pt(OOCCH_3)_2(dbtp)_2]$·dmf complex proceeded with rate constant $k_{1(solv)} = 0.71 \times 10^{-3}\ s^{-1}$ at 298 K and is faster than $[Pt(C_5F_6O_4)(dmtp)_2]$ ($0.15 \times 10^{-3}\ s^{-1}$, 300 K [26]), oxaliplatin ($0.72 \times 10^{-3}\ s^{-1}$, 310 K

Table 4. Kinetic data and activation parameters for the first step of basic hydrolysis of the Pt(II) complexes.

Complex	I (M)	T (K)	$10^3\ k_{i(OH^-)}$ ($s^{-1}\ M^{-1}$)	$10^3\ k_{1(solv)}$ (s^{-1})
$[Pt(C_5F_6O_4)(dmtp)_2]\cdot 2H_2O$[26]	0.1	300	2.5 ± 0.2	0.15 ± 0.01
		310	8.7 ± 0.6	0.34 ± 0.04
		320	20.5 ± 2.3	0.56 ± 0.20
Oxaliplatin[27]	0.5	310	0.92	0.72
Carboplatin[28]	–	310	–	$<5 \times 10^{-6}$
Cisplatin[29]	0.1	298	–	0.019
cis-$[Pt(OOCCH_3)_2(dbtp)_2]$	0.1	298	5.5 ± 1.7	0.71 ± 0.12
		303	6.9 ± 0.8	0.78 ± 0.05
		308	12.0 ± 0.6	0.79 ± 0.04
		313	16.6 ± 1.0	0.89 ± 0.06
Activation parameters[a]				
$\Delta H^{\neq}$ [kJ mol^{-1}]			57.9 ± 4	35.3 ± 5
$\Delta S^{\neq}$ [J $mol^{-1}\ K^{-1}$]			-94.5 ± 12	-183 ± 15

[a]For *cis*-$[Pt(OOCCH_3)_2(dbtp)_2]$.

Table 5. Kinetic data and activation parameters for the first step of aquation of the platinum(II) complexes in acidic media (pH 5–7, HEPES buffer).

Complex	I (M)	T (K)	$k_{i(H^+)}$ ($s^{-1}\ M^{-1}$)	$10^3\ k_{1(solv)}$ (s^{-1})
Oxaliplatin [27]	0.5	310	–	0.0012
cis-$[Pt(OOCCH_3)_2(dbtp)_2]\cdot$dmf	0.1	308	16.9 ± 2.9	1.61 ± 0.02
Cisplatin [29]	0.1	298	–	0.063

[27]), carboplatin ($<5 \times 10^{-9}\ s^{-1}$, 310 K [28]), and cisplatin ($0.019 \times 10^{-3}\ s^{-1}$ [29]). For $[Pt(C_5F_6O_4)(dmtp)_2]\cdot 2H_2O$, oxaliplatin and carboplatin, however, the first hydrolysis step is ring opening process in the chelate carboxylate, suggested to be faster than the second step of hydrolysis. These results may be contrasted with those for *trans*-acetate complexes, *trans*-$[Pt(OOCCH_3)_2(NH_3)(N)]$, where N = 2-, 3-, or 4-picoline [30, 31]. The rate constants k_1 determined from HPLC for these compounds were $1.07–3.26 \times 10^{-6}\ s^{-1}$ (310 K, $I = 0.02$ M). Thus, the k_1 value for the *trans*-$[Pt(OOCCH_3)_2(NH_3)(N)]$ complexes is slower by three orders of magnitude than the $k_{1(solv)}$ value of $0.79 \times 10^{-3}\ s^{-1}$ (308 K, $I = 0.01$ M) for (**1**). In particular, the obtained results suggested a strong *cis* labilizing effect of the mutually *cis* acetates in (**1**). Platinum(II) compound as a cytotoxic agent binds to DNA via intra-strand crosslinking, using both coordination sites in *cis* position originally occupied by leaving groups, so that hydrolysis of both carboxylate ligands is necessary. Unfortunately, the second hydrolysis process was not detectable for *cis*-$[Pt(OOCCH_3)_2(dbtp)_2]$ as for *trans*-acetate platinum(II) complexes [32].

ESI-MS spectra with positive ion mode were performed in neutral aqueous solution. Two ion peaks ($M + H^+ = 778$ *m/z*, $M + Na^+ = 800$ *m/z*), assignable on the basis of mass-to-charge ratios and isotopic models (18) correspond to (**1**) (Supplementary data: SI_3). Within 1 h, after dissolving and alkalizing the solutions of (**1**), new peaks appeared ($M + Na^+ = 758$ *m/z*), corresponding to the $[Pt(OOCCH_3)(OH)(dbtp)_2]$ (Supplementary data: SI_4). The *cis*-$[Pt(OH)_2(dbtp)_2]$ complex as a final product of hydrolysis was not identified by ESI-MS analysis. In ESI-MS spectrum with negative ion mode, no signals for the platinum(II) complex and reaction products were detected.

In ^{13}C NMR spectra of (**1**) in basic D_2O solution (pH 12, 0.01 g NaOH in 1 mL), characteristic resonance peaks, attributed to dbtp carbons, disappeared and the only peak assigned

to the free acetate was observed in 48 h. On the basis of ^{13}C NMR analysis of the reaction mixture of platinum(II) complex with hydroxide in D_2O, it can be assumed that the leaving group in hydrolysis is acetate. Some precipitates occurred under such circumstances, at higher concentrations of complex (5×10^{-3} M) in aqueous solution used in the NMR analysis. A possible explanation could be a formation of polynuclear oligomers by hydroxo ions as products of hydrolysis, which cannot be further identified by this technique.

As in the case of the dicarboxylate complex $[Pt(C_5F_6O_4)(dmtp)_2]\cdot 2H_2O$ [26], the acetate complex of platinum(II) with dbtp in solution shows a large affinity for basic hydrolysis and the magnitude of this effect is dependent on the nature of the leaving groups as well as non-leaving amine ligands. The lability of monofunctional carboxylate is greater than that of chelate oxalate (oxaliplatin) and chloride (cisplatin). It seems that coordination of the biomolecules, such as dbtp, should enhance the selectivity of these antitumor drugs, which activity can be estimated on the basis of biological studies as well as kinetic research.

3.5. *Cytotoxicity*

Results of the *in vitro* cytotoxicity assays against A549, T47D, FaDu, and A2780cis of *cis*-$[Pt(OOCCH_3)_2(dbtp)_2]\cdot$dmf (**1**) are summarized in table 6. The obtained results were compared to those of cisplatin, carboplatin, and oxaliplatin. (**1**) displayed significant *in vitro* cytotoxic activity against all cancerous cell lines with IC_{50} values of 0.26–1.80 μM. (**1**) had even 56- or 70-fold lower IC_{50} value toward T47D than cisplatin and oxaliplatin. Against cisplatin-resistant ovarian cancer cells (A2780cis), (**1**) showed remarkable potency (IC_{50} = 1.80 μM) and exhibited greater than six and fifty-six times the activity of cisplatin and carboplatin, respectively. The cytotoxicity of (**1**) was slightly weaker than oxaliplatin, however, the improved activity of *cis*-$[Pt(OOCCH_3)_2(dbtp)_2]\cdot$dmf toward both cisplatin-resistant breast (T47D) as well as ovarian (A2780cis) cancer cell lines indicates the ability to overcome cisplatin resistance in these tumor cells. Furthermore, (**1**) was at least fivefold more active compared to cisplatin and oxaliplatin in the human pharyngeal squamous carcinoma (FaDu) as well as human lung adenocarcinoma (A549) cell lines.

The impact of the carrier ligand on *in vitro* cytotoxicity of platinum(II) compounds containing dbtp has been discussed [11]. In the case of both compared tumor cell lines (A549 and T47D), the acetate complex was found to be the most efficient in killing cancerous cells. Toward T47D, the ranking of the *in vitro* activity was followed by acetate (0.26 μM), chloride (1.50 μM), nitrate (2.30 μM), malonate (2.66 μM), iodide (4.80 μM), and malate (5.30 μM). The platinum(II) acetate complex (**1**) was 10-fold more potent than

Table 6. Partition coefficient (log *P*) and *in vitro* antiproliferative activity of Pt(II) complexes.

		IC_{50} (μM)[b]				
Complex	log *P*[a]	A549	T47D	FaDu	A2780cis	BALB/3T3
(**1**)	1.66	0.62 ± 0.41	0.26 ± 0.06	0.53 ± 0.34	1.80 ± 0.75	3.27 ± 1.68
Carboplatin	–1.48[33]	150.56 ± 53.06	uv[c]	45.39 ± 11.50	98.08 ± 4.08	14.30 ± 6.68
Cisplatin	–1.76	9.00 ± 1.00	14.43 ± 1.90	2.83 ± 1.00	10.97 ± 0.57	3.17 ± 1.47
Oxaliplatin	–1.65[33]	4.15 ± 2.79	18.28 ± 7.06	4.54 ± 1.77	1.45 ± 0.17	2.38 ± 0.01

[a]The values are averages of five independent determinations.
[b]Further details on these assays are given in the Experimental section. Data represent the mean of at least three independent experiments (n = 3–5); the values ± SD are given.
[c]Unavailable in the range of concentrations used; IC_{50} could not be calculated due to weak antiproliferative activity of compound across the tested concentrations.

Table 7. The selectivity factor (SF) which represents IC_{50} for normal cell line/IC_{50} for cancerous.

	Tumor cell line			
Complex	A549	T47D	FaDu	A2780cis
cis–[Pt(OOCCH$_3$)$_2$(dbtp)$_2$]·dmf (**1**)	5.27	12.58	6.29	1.82
Carboplatin	0.09	–	0.32	0.15
Cisplatin	0.35	0.22	1.12	0.29
Oxaliplatin	0.57	0.13	0.52	1.64

Notes: The SF (selectivity factor) was calculated for each compound using formula: SF = IC_{50} for normal cell line, (BALB/3T3)/IC_{50} for respective cancerous cell lines. A beneficial SF > 1.00 indicates a drug with efficacy against tumor cells greater than toxicity against normal cells.

the malonate analog. The *in vitro* activity of the tested compounds against A549 is in the order: *cis*-[Pt(OOCCH$_3$)$_2$(dbtp)$_2$]·dmf (0.62 μM) > [Pt(malonate)(dbtp)$_2$] (4.00 μM) and [Pt(malate)(dbtp)$_2$] (4.80 μM) > *cis*-[PtCl$_2$(dbtp)$_2$] (6.20 μM) > *cis*-[Pt(NO$_3$)$_2$(dbtp)$_2$] (6.90 μM) > *cis*-[PtI$_2$(dbtp)$_2$] (7.90 μM). Furthermore, despite the pronounced cytotoxicity of dichlorido [15] counterpart against A549 and T47D tumor cells, its antiproliferative ability was found to be nine to sixfold less potent than *cis*-[Pt(OOCCH$_3$)$_2$(dbtp)$_2$]·dmf.

In the quest for less toxic platinum drugs, an investigation of the antiproliferative *in vitro* activity against normal cells is necessary. Thus, the *in vitro* toxicity toward normal mouse embryonic fibroblast cells was estimated (table 6). (**1**) exhibited lower potencies than cisplatin as well as oxaliplatin, however, (**1**) revealed greater ability to inhibit the proliferation of BALB/3T3 compared to carboplatin. Overall, the number of cells killed by the tested compounds increased: carboplatin < *cis*-[Pt(OOCCH$_3$)$_2$(dbtp)$_2$]·dmf < cisplatin < oxaliplatin.

A very serious problem of the commonly used chemotherapeutics is their non-selective activity. Drugs are often toxic to both tumor and normal cells. To calculate a selectivity factor (SF) for the Pt(II) complexes, the IC_{50} values against normal mouse embryonic fibroblast cells (BALB/3T3) were compared with the IC_{50} values of each cancer cell line (the quotient between the IC_{50} for the normal BALB/3T3 cell line and the IC_{50} for each cancerous cells) (table 7). A value >1.00 is considered selective for activity against tumor cells [11, 34–36]. Despite rather low IC_{50} values toward BALB/3T3, *in vitro* cytotoxic *cis*-[Pt(OOCCH$_3$)$_2$(dbtp)$_2$]·dmf demonstrated higher selectivity (SF > 1.00) for all tested cancer cell lines than for mouse fibroblast cells. The computed SFs for this compound were higher than those of cisplatin, carboplatin, and oxaliplatin (table 7). It should be emphasized that against cisplatin-resistant human breast tumor cells (T47D), (**1**) was at least 56-fold more selective than cisplatin and oxaliplatin. Using acetate led to a significantly cytotoxic and highly selective antiproliferative agent for cancer treatment.

3.6. *Lipophilicity*

Lipophilicity is an important physicochemical property related to drug absorption in the gastrointestinal track [37]. To evaluate the lipophilicity of *cis*-[Pt(OOCCH$_3$)$_2$(dbtp)$_2$]·dmf, its partition coefficients between *n*-octanol and water were measured. The obtained value (log = 1.66) indicates that (**1**) is more lipophilic than cisplatin, carboplatin, or oxaliplatin (table 6).

The resistance to cisplatin has been identified as decreased drug accumulation, increased cytoplasmic detoxification, and increased DNA repair [38, 39]. More lipophilic drugs assist

in circumventing cisplatin resistance by an increase in passive diffusion through the cell membrane rather than relying on an active uptake [40]. It is generally known that drugs with higher lipophilicity are more permeable through the cell membrane and accordingly absorbed more efficiently in the digestive tract, whereas hydrophilic drugs are not well absorbed. However, highly lipophilic drugs showed low absorption efficiency due to their poor water solubility, too.

In the case of the obtained Pt(II) acetate complex, the significant cytotoxicity can be also related to lipophilicity. The *cis*-[Pt(OOCCH$_3$)$_2$(dbtp)$_2$]·dmf exhibited moderate hydrophobic character, which suggests that they should cross cell membranes using passive diffusion.

The influence of lipophilicity on the cytotoxic properties of malonate platinum(II) complexes with disubstituted 1,2,4-triazolo[1,5-*a*]pyrimidines has been reported [11]. An increase in the *in vitro* cytotoxicity against several cancer cell lines was observed as log *P* increased. In comparison to the previously published [Pt(malonate)(dbtp)$_2$] (log = 2.07), a substitution of bidendate malonate by acetate resulted in a decrease in the log *P* value and an increase in the *in vitro* activity. Our results suggest that using two *cis* monodentate carboxylates significantly improves the therapeutic profile of a new drug candidate *cis*-[Pt(OOCCH$_3$)$_2$(dbtp)$_2$]·dmf.

4. Concluding remarks

A new lipophilic *cis*-diacetate platinum(II) complex with two monodentate 5,7-ditertbutyl-1,2,4-triazolo[1,5-*a*]pyrimidine (dbtp) ligands has been synthesized and characterized. In the solution ($CDCl_3$), the coordination compound forms two rotamers with a different arrangement of triazolopyrimidines, head-to-tail (**1a**), and head-to-head (**1b**). Computational studies confirmed that (**1a**) is energetically more stable than (**1b**). Kinetic studies showed that the first hydrolysis step of (**1**) is faster than platinum(II) drugs (cisplatin, carboplatin, and oxaliplatin), which may be related to its *in vitro* activity. Additionally, *cis*-[Pt(OOCCH$_3$)$_2$(dbtp)$_2$]·dmf (**1**) exhibited significant ability to inhibit the growth of all tested cancer cell lines. Notably, (**1**) overcame the cisplatin-resistance mechanism in the breast (T47D) as well as ovarian (A2780cis) cancer cells. Moreover, comparing the *in vitro* cytotoxicity and toxicity of *cis*-acetate platinum(II) complex, (**1**) was at least 56-fold more selective against T47D than cisplatin and oxaliplatin. The improved therapeutic profile of *cis*-[Pt(OOCCH$_3$)$_2$(dbtp)$_2$]·dmf indicates that it has much promise as an antitumor agent for future investigation.

Supplementary information

SI_1. Spectroscopic data for (**1a**) and (**1b**).

SI_2. Observed rate constants for initiated process (k_{1obs}) and first step of hydrolysis of *cis*-[Pt(OOCCH$_3$)$_2$(dbtp)$_2$] (k_{2obs}) and standard errors (s_i).

SI_3. ESIMS mass spectra of *cis*-[Pt(OOCCH$_3$)$_2$(dbtp)$_2$]·dmf in H_2O (immediately after dissolving).

SI_4. ESIMS mass spectra of *cis*-[Pt(OOCCH$_3$)$_2$(dbtp)$_2$]·dmf in sodium hydroxide solution (1 h after dissolving).

Acknowledgements

The authors wish to thank the Wroclaw Centre for Networking and Supercomputing, and the Academic Computer Centre Cyfronet AGH Cracow for generous allotment of computational facilities.

Disclosure statement

No potential conflict of interest was reported by the authors.

Supplemental data

Supplemental data for this article can be accessed here [http://dx.doi.org/10.1080/00958972.2015.1070954].

ORCID

Kamil Hoffmann http://orcid.org/0000-0002-9259-7857

References

[1] J.M. Balkaran, S.C.P. van Bezouw, J. van Bruchem, J. Verasdonck. *Inorg. Chim. Acta*, **362**, 861 (2009).
[2] A.B. Caballero, C. Marín, A. Rodríguez-Diéguez, I. Ramírez-Macías, E. Barea, M. Sánchez-Moreno, J.M. Salas. *J. Inorg. Biochem.*, **105**, 770 (2011).
[3] M. Abul Haj, M. Quirós, J.M. Salas. *Polyhedron*, **23**, 2373 (2002).
[4] J.M. Salas, M. Angustias Romero, M.O. Purificación Sánchez, M. Quirós. *Coord. Chem. Rev.*, **193–195**, 1119 (1999).
[5] E. Günay, I. Mutikainen, U. Turpeinen, G.A. van Albada, J.G. Haasnoot, J. Reedijk. *J. Chem. Crystallogr.*, **40**, 1006 (2010).
[6] J.M. Balkaran, S.C.P. van Bezouw, J. van Bruchem, J. Verasdonck, P.C. Verkerk, A.G. Volbeda, I. Mutikainen, U. Turpeinen, G.A. van Albada, P. Gamez, J.G. Haasnoot, J. Reedijk. *Inorg. Chim. Acta*, **362**, 861 (2009).
[7] I. Łakomska, H. Kooijman, A.L. Spek, W.-Z. Shen, J. Reedijk. *Dalton Trans.*, **48**, 10736 (2009).
[8] I. Łakomska, M. Fandzloch, T. Muzioł, T. Lis, J. Jezierska. *Dalton Trans.*, **42**, 6219 (2013).
[9] E. Szłyk, A. Grodzicki, L. Pazderski, I. Sitkowski. *Pol. J. Chem.*, **72**, 55 (1998).
[10] E. Szłyk, A. Grodzicki, L. Pazderski, A. Wojtczak, J. Chatłas, G. Wrzeszcz, J. Sitkowski, B. Kamieński. *J. Chem. Soc., Dalton Trans.*, 867 (2000).
[11] I. Łakomska, K. Hoffmann, A. Wojtczak, J. Sitkowski, E. Maj, J. Wietrzyk. *J. Inorg. Biochem.*, **141**, 188 (2014).
[12] I. Łakomska, M. Fandzloch, T. Muzioł, J. Sitkowski, J. Wietrzyk. *J. Inorg. Biochem.*, **100**, 115 (2012).
[13] I. Łakomska, E. Szłyk, J. Sitkowski, L. Kozerski, J. Wietrzyk, M. Pełczyńska, A. Nasulewicz, A. Opolski. *J. Inorg. Biochem.*, **98**, 167 (2004).
[14] I. Łakomska, A. Wojtczak, J. Sitkowski, L. Kozerski, E. Szłyk. *Polyhedron*, **27**, 2765 (2008).
[15] I. Łakomska. *Inorg. Chim. Acta*, **362**, 669 (2009).
[16] C. Bülow, K. Haas. *Berichte*, **42**, 4638 (1909).
[17] M.J. Frisch, G.W. Trucks, H.B. Schlegel, G.E. Scuseria, M.A. Robb, J.R. Cheeseman, G. Scalmani, V. Barone, B. Mennucci, G.A. Petersson, H. Nakatsuji, M. Caricato, X. Li, H.P. Hratchian, A.F. Izmaylov, J.Bloino, G. Zheng, J.L. Sonnenberg, M. Hada, M. Ehara, K. Toyota, R. Fukuda, J. Hasegawa, M. Ishida, T. Nakajima, Y. Honda, O. Kitao, H. Nakai, T. Vreven, J.A. Montgomery Jr, J.E. Peralta, F. Ogliaro, M. Bearpark, J.J. Heyd, E. Brothers, K.N. Kudin, V.N. Staroverov, R. Kobayashi, J. Normand, K. Raghavachari, A. Rendell, J.C. Burant, S.S. Iyengar, J. Tomasi, M. Cossi, N. Rega, J.M. Millam, M. Klene, J.E. Knox, J.B. Cross, V. Bakken, C. Adamo, J. Jaramillo, R. Gomperts, R.E. Stratmann, O. Yazyev, A.J. Austin, R. Cammi, C. Pomelli, J.W. Ochterski, R.L. Martin, K. Morokuma, V.G. Zakrzewski, G.A. Voth, P. Salvador, J.J. Dannenberg, S. Dapprich, A.D. Daniels, Ö. Farkas, J.B. Foresman, J.V. Ortiz, J. Cioslowski, D.J. Fox, *Gaussian 09, Revision D.01*, Gaussian, Inc., Wallingford, CT (2009).
[18] D. Figgen, K.A. Peterson, M. Dolg, H. Stoll. *J. Chem. Phys.*, **130**, 164108 (2009).

[19] P. Skehan, R. Storeng, D. Scudiero, A. Monks, J. McMahon, D. Vistica, J.T. Warren, H. Bokesch, S. Kenney, M.R. Boyd. *J. Natl. Cancer Inst.*, **82**, 1107 (1990).
[20] A. Albert (Ed.). *Selective Toxicity. The Physico-Chemical Basis of Therapy*, pp. 662–664, Chapman and Hall, London (1979).
[21] I. Łakomska, M. Barwiołek, A. Wojtczak, E. Szłyk. *Polyhedron*, **26**, 5349 (2007).
[22] G.B. Deacon, R.J. Phillips. *Coord. Chem. Rev.*, **33**, 227 (1980).
[23] Z. Dhaouadi, M. Ghomi, J.C. Austin, R.B. Girling, R.E. Hester, P. Mojzes, L. Chinsky, P.Y. Turpin, C. Coulombeau. *J. Phys. Chem.*, **97**, 1074 (1993).
[24] S. Roy, J.A. Westmaas, F. Buda, J. Reedijk. *J. Inorg. Biochem.*, **103**, 1278 (2009).
[25] J.R. Wenner, V.A. Bloomfield. *Anal. Biochem.*, **268**, 201 (1999).
[26] I. Łakomska, K. Hoffmann, A. Topolski, T. Kloskowski, T. Drewa. *Inorg. Chim. Acta*, **387**, 455 (2012).
[27] E. Jerremalm, P. Videhult, G. Alvelius, W.J. Griffiths, T. Bergman, S. Eksborg, H. Ehrsson. *J. Pharm. Sci.*, **91**, 189 (2002).
[28] U. Frey, J.D. Ranford, P.J. Sadler. *Inorg. Chem.*, **32**, 1333 (1993).
[29] S.E. Miller, D.A. House. *Inorg. Chim. Acta*, **166**, 189 (1989).
[30] G.H. Bulluss, K.M. Knott, E.S.F. Ma, S.M. Aris, E. Alvarado, N. Farrell. *Inorg. Chem.*, **45**, 5733 (2006).
[31] S.M. Aris, N.P. Farrell. *Eur. J. Inorg. Chem.*, **10**, 1293 (2009).
[32] E.S.F. Ma, W.D. Bates, A. Edmunds, L.R. Kelland, T. Fojo, N. Farrell. *J. Med. Chem.*, **48**, 5651 (2005).
[33] I.V. Tetko, I. Jaroszewicz, J.A. Platts, J. Kuduk-Jaworska. *J. Inorg. Biochem.*, **102**, 1424 (2008).
[34] M. Alessio, I. Zanellato, I. Bonarrigo, E. Gabano, M. Ravera, D. Osella. *J. Inorg. Biochem.*, **129**, 52 (2013).
[35] A.B. Caballero, A. Rodríguez-Diéguez, J.M. Salas, M. Sánchez-Moreno, C. Marín, I. Ramírez-Macías, N. Santamaría-Díaz, R. Gutiérrez-Sánchez. *J. Inorg. Biochem.*, **138**, 39 (2014).
[36] A. Huczyński, J. Rutkowski, I. Borowicz, J. Wietrzyk, E. Maj, B. Brzezinski. *Bioorg. Med. Chem. Lett.*, **23**, 5053 (2013).
[37] B. Lippert (Ed.). *Cisplatin. In the Development of Orally Active Platinum Drugs*, pp. 497–521, Wiley-VCH, Weinheim (1999).
[38] L.R. Kelland. *Eur. J. Cancer.*, **30**, 725 (1994).
[39] R.P. Perez. *Eur. J. Cancer.*, **34**, 1535 (1998).
[40] M.D. Hall, T.W. Hambley. *Coord. Chem. Rev.*, **232**, 49 (2002).